

INSTRUCTTA: Instruction-Tuned Targeted Attack for Large Vision-Language Models

Xunguang Wang¹, Zhenlan Ji¹, Pingchuan Ma¹, Zongjie Li¹, and Shuai Wang¹

The Hong Kong University of Science and Technology, Hong Kong, China
{xwanghm, zjiae, pmaab, zligo, shuaiw}@cse.ust.hk

Abstract. Large vision-language models (LVLMs) have demonstrated their incredible capability in image understanding and response generation. However, this rich visual interaction also makes LVLMs vulnerable to adversarial examples. In this paper, we formulate a novel and practical targeted attack scenario that the adversary can only know the vision encoder of the victim LVLM, without the knowledge of its prompts (which are often proprietary for service providers and not publicly available) and its underlying large language model (LLM). This practical setting poses challenges to the cross-prompt and cross-model transferability of targeted adversarial attack, which aims to confuse the LVLM to output a response that is semantically similar to the attacker’s chosen target text. To this end, we propose an instruction-tuned targeted attack (dubbed INSTRUCTTA) to deliver the targeted adversarial attack on LVLMs with high transferability. Initially, we utilize a public text-to-image generative model to “reverse” the target response into a target image, and employ GPT-4 to infer a reasonable instruction p' from the target response. We then form a local surrogate model (sharing the same vision encoder with the victim LVLM) to extract instruction-aware features of an adversarial image example and the target image, and minimize the distance between these two features to optimize the adversarial example. To further improve the transferability with instruction tuning, we augment the instruction p' with instructions paraphrased from GPT-4. Extensive experiments demonstrate the superiority of our proposed method in targeted attack performance and transferability. The code is available at <https://github.com/xunguangwang/InstructTA>.

1 Introduction

Large vision-language models (LVLMs) have achieved great success in text-to-image generation [41], image captioning [9], visual question-answering [28], visual dialog [21], etc., due to the colossal increase of training data and model parameters. Benefiting from the strong comprehension of large language models (LLMs), recent LVLMs [2–4, 14, 21, 28, 32, 46, 57] on top of LLMs have demonstrated a superior capability in solving complex tasks than that of small vision-language models. It is noted that GPT-4 [37] supports visual inputs and performs human-like conversations in various complicated scenarios.

However, recent studies [5, 16, 42, 55] exposed that LLMs with visual structures could be easily fooled by adversarial examples (AEs) crafted via adding imperceptible perturbations to benign images. In particular, targeted attack with malicious goals raises more serious safety concerns for LVLMs and their downstream applications. For example, targeted adversarial examples could jailbreak LVLMs to explain the bomb-making process or trick medical diagnostic models into generating reports of specific diseases for insurance. It is thus demanding to comprehensively study adversarial attacks on LVLMs to address these security threats before safety breaches happen.

This paper focuses on the targeted attack on LVLMs, where the adversary aims to generate an adversarial image that misleads the LVLM to respond with a specific target text, despite varying instructions the LVLM may use. Typically, LVLMs are deployed by service providers for vertical applications in the cloud, and the built-in prompts¹ and the parameters of LLMs leveraged by the LVLMs are not publicly accessible as they are proprietary to the service providers. Conversely, it is reasonable to assume that attackers possess knowledge of the vision encoder in the LVLM, as developers often disclose the structure of the model in technical reports or attackers can acquire this information through social engineering. Consequently, adversaries can easily construct surrogate models with the same vision encoders to facilitate attacks. Nonetheless, the uncertainty surrounding the LVLM model itself and its internal instructions presents challenges for targeted attacks: (1) The attacker cannot easily gain the instruction-aware features from the vision encoder to launch exact targeted attacks due to a lack of instructions. (2) Cross-model and cross-instruction transferability places new demands on the targeted attack, since the victim LVLM may have distinct LLM backends and use varying (unknown) instructions.

To overcome these challenges, this paper proposes an instruction-tuned targeted attack (INSTRUCTTA) for LVLMs with high attack transferability. As depicted in Fig. 1, we first employ GPT-4 [37] to infer an instruction \mathbf{p}' in line with the attacker-decided response, and also generate a target image for the target response using a text-to-image generative model. Subsequently, we take both images and instructions as inputs to a local surrogate model to extract informative features tailored to the target response. INSTRUCTTA then minimizes the feature distance between the adversarial image example and the target image. Moreover, INSTRUCTTA rephrases \mathbf{p}' into a set of instructions with close semantics, and leverages them to effectively improve the transferability of generated adversarial samples. Our main contributions are outlined as follows:

- We propose an effective targeted attack, INSTRUCTTA. It cleverly leverages LLMs to deduce reasonable prompts for target texts, leading to extracting instruction-aware features for precise targeted attacks.
- We present the instruction-tuning paradigm in the targeted attacks to further augment the transferability of adversarial samples, benefiting from the rephrased instructions by GPT-4.

¹ To clarify, in this paper, we use the term “instruction” and “prompt” interchangeably.

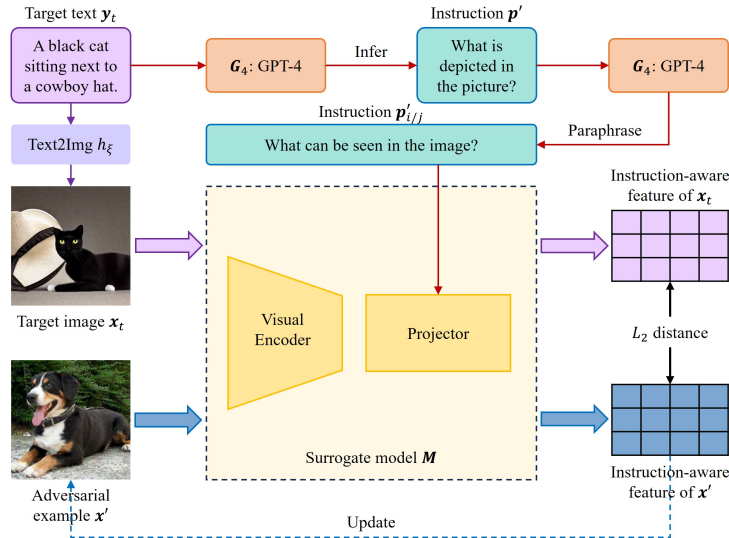


Fig. 1: The framework of our instruction-tuned targeted attack (INSTRUCTTA). Given a target text y_t , we first transform it into the target image x_t with a text-to-image model h_ξ . Simultaneously, GPT-4 infers a reasonable instruction p' . Upon providing the augmented instruction p'_i and p'_j which are rephrased from p' using GPT-4, the surrogate model M extracts instruction-aware features of x_t and the AE x' , respectively. Finally, we minimize the L_2 distance between these two features to optimize x' .

- Extensive experiments demonstrate that INSTRUCTTA can achieve better targeted attack performance and transferability than intuitive baselines. We also discuss mitigations and ethics considerations of INSTRUCTTA.

2 Related Work

LVLMS. Benefiting from the powerful capabilities of LLMs in answering diverse and complex questions [36], LVLMS [55] have demonstrated remarkable performance on a variety of multi-modal tasks, *e.g.*, image captioning, visual question-answering, natural language visual reasoning, and visual dialog. To bridge the image-text modality gap, BLIP-2 [28] proposes the Q-Former to extract visual features into the frozen OPT [54] or FlanT5 [13]. MiniGPT-4 [57] employs the identical pre-trained ViT [18] and Q-Former as BLIP-2 but uses the more powerful Vicuna [12] to serve as the base LLM for text generation. InstructBLIP [14] introduces an instruction-aware Q-Former to extract the most task-relevant visual representations. LLaVA [32] bridges a pre-trained visual encoder with LLaMA, and fine-tunes them with question-image-answer paired data generated by GPT-4. Instead of projecting visual features onto the input embedding space of the LLM, CogVLM [46] introduces a visual expert module to

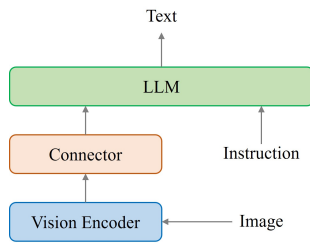


Fig. 2: The architecture of LVLm.

synergistically incorporate image and linguistic features within the pre-trained large language model.

Adversarial Attacks. Although adversarial attacks are now being developed in a variety of modalities and tasks, the earliest and most extensive research occurred in the field of image classification [6, 44]. In this case, the goal of the adversarial attack is often to fool a well-trained visual classifier by crafted adversarial images. Based on their purpose, we divide adversarial attacks into *targeted attacks* and *non-targeted attacks* [1]. Targeted attacks aim to confuse the model to recognize the adversarial example as a target label, whereas non-targeted attacks only ensure that the model makes wrong predictions, not caring about the output error category. Moreover, according to the information of the attacked model exposed to the adversary, adversarial attacks can be grouped into white-box attacks and black-box attacks. The white-box attacks can obtain the whole parameters and structure of the target model. Thus, they generally optimize adversarial perturbations with gradients of loss *w.r.t* inputs, *e.g.*, FGSM [22], I-FGSM [26], C&W [7] and PGD [35]. In contrast, only the input and output of the attacked model can be captured by black-box attacks, which is more challenging and practical than white-box one. One solution is to estimate the gradient or search for successful perturbations by directly querying the target model multiple times, *e.g.*, ZOO [10] and NES attack [25]. Another way is to implement *transfer attacks* by constructing adversarial samples from substitute models, *e.g.*, SBA [39] and ensemble-based approaches [17, 20, 24, 33].

Besides image classification, researchers have extended adversarial attacks to vision-language models or tasks [8, 27, 31, 34, 45, 47–50, 52, 56]. Recently, investigating adversarial robustness on vision-language pre-training (VLP) models [34, 47, 52] has aroused much attention. Zhang *et al.* [52] proposed Co-Attack for VLP models, which collaboratively combines the image and the text perturbations. SGA [34] improved the adversarial transferability across different VLP models by breaking the set-level cross-modal alignment.

AEs on LVLms. Currently, there are some pioneering works of targeted attacks on LVLms. On one hand, some works aim to mislead the LVLms to output specific words. For example, Bailey *et al.* [5] forces the LVLm to respond with the target string in a white-box setting. Dong *et al.* [16] present text description attack to mislead the black-box Bard [23] to output targeted responses, which

maximize the log-likelihood of the substitute LVLMs to predict the target sentence. On the other hand, some works have been devoted to fooling LVLMs into outputting text with the same semantics as the target. For example, Zhao *et al.* [55] propose three feature matching methods (*i.e.*, MF-it, MF-ii and MF-tt) to launch targeted attack with given target text against LVLMs in black-box settings. Shayegani *et al.* [42] also align the adversarial image and target images in the embedding space for LVLM jailbreak. Different from [55], we further improve the attack transferability under the guidance of inferred and rephrased instructions. While [42] jailbreaks LVLMs with a generic prompt by perturbing the input image, our work highlights the capability to implement targeted attacks even without knowing the built-in prompts of the target LVLM.

3 Method

3.1 Problem Formulation

LVLM. Given an image \mathbf{x} and a text prompt \mathbf{p} as inputs, the LVLM F outputs an answer \mathbf{y} . Formally,

$$\mathbf{y} = F_{\theta}(\mathbf{x}, \mathbf{p}), \quad (1)$$

where F_{θ} denotes the LVLM parameterized by θ . Typically, the LVLM [14, 28, 32, 57] projects the extracted visual features into the word embedding space and then feeds them to its underlying LLM. Hence, LVLM consists of a pre-trained vision encoder, a connector and a well-trained LLM, as shown in Fig. 2.

Adversarial Objective. In image-grounded text generation, the goal of targeted attack is to construct adversarial examples, which could cause the output of the victim model to match a predefined targeted response. Under the L_{∞} norm constraint, the objective of a targeted attack can be formulated as follows:

$$\begin{aligned} \Delta(\mathbf{x}, \mathbf{y}_t) &:= \max_{\mathbf{x}'} S(F(\mathbf{x}', \mathbf{p}), \mathbf{y}_t), \\ \text{s.t. } &\|\mathbf{x}' - \mathbf{x}\|_{\infty} \leq \epsilon, \end{aligned} \quad (2)$$

where \mathbf{x} is a given benign image, \mathbf{x}' represents the adversarial example of \mathbf{x} , and \mathbf{y}_t denotes the predefined target text. ϵ is the budget of controlling adversarial perturbations, and \mathbf{p} denotes the instruction used by the target LVLM (\mathbf{p} is unknown to attackers; see § 3.2). $S(\cdot, \cdot)$ is a metric depicting the semantic similarity between two input sentences. This way, Eqn. 2 ensures that the response of the adversarial example shall retain the same meaning as the target text \mathbf{y}_t .

3.2 Targeted Attack with Instruction Tuning

Assumption. In this paper, we consider a practical gray-box setting, where the adversary only knows the visual encoder used in the attacked model, excluding LLMs and instructions of the victim LVLM. That is, the adversary is agnostic to \mathbf{p} . Instead, we assume that attackers know the usage domain of the target LVLM, *e.g.*, CT image diagnosis; considering F is often hosted as a task-specific

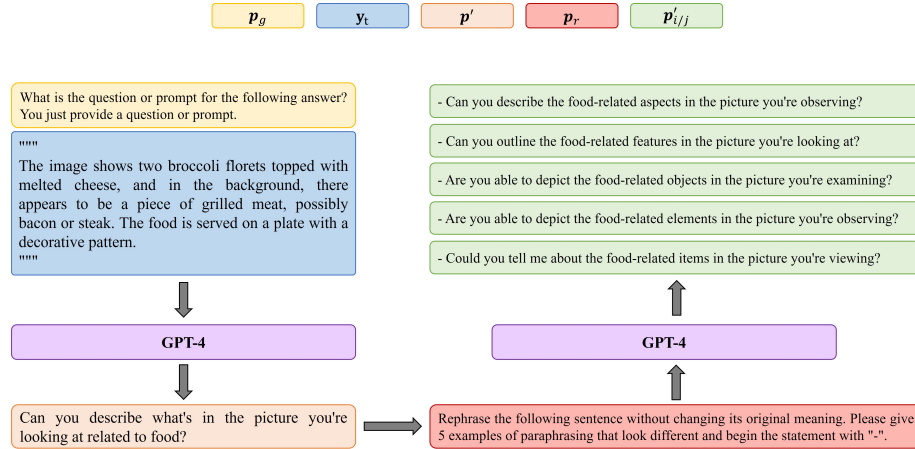
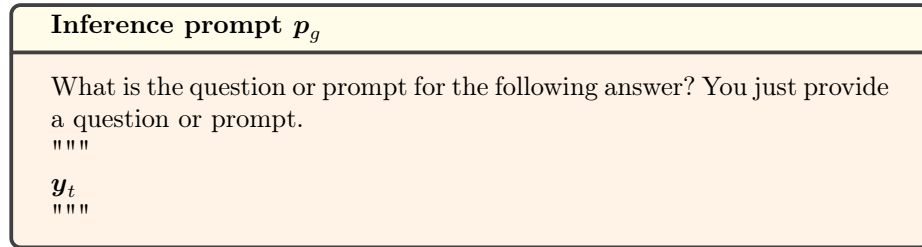


Fig. 3: An example of rephrasing an instruction. Given the target response y_t , GPT-4 infers an instruction, *i.e.*, “Can you describe what’s in the picture you’re looking at related to food?”. The real instruction assigned to this target text is “What are the essential components depicted in this image?”

service, attackers can easily obtain this information. Accordingly, attackers can locally prepare instructions p' which are commonly used in the target domain (see below for details). We also assume that before attack, attackers can form a local surrogate model with the same vision encoder as that of the victim model. **Inferring Instructions.** We first locally infer the possible instruction p' for the target text y_t by using GPT-4 [37]. We design the inference prompt p_g as follows.



According to the above prompt, we can derive a reasonable instruction p' by feeding the target response text y_t to GPT-4.

Forming Surrogate Models. The surrogate model comprises two modules: the visual encoder sourced from the victim model and the pre-trained projector. The projector follows the visual encoder, as depicted in Fig. 1. By providing an instruction as input, the projector is capable of mapping the existing global features into informative features that are specifically tailored to the given instruction. In this paper, Q-Former [28] is selected as the projector. Consequently, once the instructions have been inferred, the surrogate model employs the projector

to convert the features obtained from the visual encoder into instruction-aware features.

Generating Adversarial Examples. We then extract the instruction-aware visual features most conducive to the task by inputting both images and the generated instructions to the surrogate model. For the targeted attack, a simple solution is to align the adversarial example to the target text in the feature space of the substitute model. Given that the surrogate model only extracts visual features, it fails to build target embedding for the target text. An alternative approach is to transform the target text into the target image through text-to-image generative models (*e.g.*, Stable Diffusion [41]). Hence, we reduce the embedding distance between the adversarial example and the target image \mathbf{x}_t for the targeted attack as:

$$\min_{\mathbf{x}'} \|M(\mathbf{x}', \mathbf{p}') - M(h_\xi(\mathbf{y}_t), \mathbf{p}')\|_2^2, \quad \text{s.t. } \|\mathbf{x}' - \mathbf{x}\|_\infty \leq \epsilon \quad (3)$$

where $M(\cdot, \cdot)$ denotes the substitute model, h_ξ is a public generative model ($\mathbf{x}_t = h_\xi(\mathbf{y}_t)$), and \mathbf{x}' indicates the adversarial sample of \mathbf{x} .

Augmenting Transferability. Our tentative exploration shows that AEs generated by Eqn. 3, although manifesting reasonable attackability, are often less transferable to the wide range of possible instructions in the wild. Thus, to improve the transferability and robustness of the generated adversarial examples, we use GPT-4 to rephrase the inferred \mathbf{p}' as augmentation. The prompt \mathbf{p}_r for paraphrasing is formulated as follows.

Rephrasing prompt \mathbf{p}_r

Rephrase the following sentence without changing its original meaning. Please give $n - 1$ examples of paraphrasing that look different and begin the statement with "-".

"""

\mathbf{p}'

"""

where $n - 1$ represents the number of sentences rephrased by GPT-4. Together with the original inferred instruction \mathbf{p}' , a total of n instructions are collected in a set Q . We set n to 10 by default. Benefiting from the augmented instructions, Eqn. 3 can be rewritten as

$$\min_{\mathbf{x}'} \mathcal{J}_{ins} = \mathbb{E}_{\mathbf{p}'_i, \mathbf{p}'_j \in Q} \|M(\mathbf{x}', \mathbf{p}'_i) - M(h_\xi(\mathbf{y}_t), \mathbf{p}'_j)\|_2^2, \quad (4)$$

s.t. $\|\mathbf{x}' - \mathbf{x}\|_\infty \leq \epsilon,$

where \mathbf{p}'_i and \mathbf{p}'_j are randomly selected from the set Q . We utilize the rephrasing prompt \mathbf{p}_r to construct the instruction set Q via GPT-4. As illustrated in Fig. 3, GPT-4 is generally effective to rephrase a seed instruction \mathbf{p}' into a set of semantically-correlated instructions.

Algorithm 1 INSTRUCTTA

Input: a benign image \mathbf{x} , a target text \mathbf{y}_t , a text-to-image generative model h_ξ , a surrogate model M , a VLP model with the visual encoder f and text encoder g , GPT-4 G_4 , custom prompts \mathbf{p}_g and \mathbf{p}_r , step size η , perturbation budget ϵ , attack iterations T

- 1: **Initialize:** $\mathbf{x}' = \mathbf{x}$,
 $\mathbf{x}_t = h_\xi(\mathbf{y}_t)$, // generate a target image
 $\mathbf{p}' = G_4(\mathbf{p}_g \mathbf{y}_t)$, //infer an instruction
 $Q \leftarrow G_4(\mathbf{p}_r \mathbf{p}')$ // build an instruction set Q by rephrasing \mathbf{p}'
- 2: **for** $iter = 1 \dots T$ **do**
- 3: $\mathbf{p}'_i \sim Q, \mathbf{p}'_j \sim Q$ // randomly select instructions
- 4: $\mathcal{L} = \mathcal{J}_{ins} - \mathcal{J}_{mf}$ // Eqn. 5
- 5: $\mathbf{x}' = \mathcal{S}_\epsilon(\mathbf{x}' - \eta \cdot \text{sign}(\Delta_{\mathbf{x}'} \mathcal{L}))$ // PGD
- 6: **end for**

Output: adversarial example \mathbf{x}'

3.3 Dual Targeted Attack & Optimization

With the aforementioned steps, we form the following dual targeted attack framework:

$$\arg \min_{\mathbf{x}'} \mathcal{L} = \mathcal{J}_{ins} - \mathcal{J}_{mf}, \quad \text{s.t. } \|\mathbf{x}' - \mathbf{x}\|_\infty \leq \epsilon, \quad (5)$$

where \mathcal{J}_{mf} is the objective of MF-it, following [55]. MF-it achieves transfer targeted attack via matching the embeddings of the adversarial example and the target response. For MF-it, its objective is defined as

$$\mathcal{J}_{mf} = [f(\mathbf{x}')]^T g(\mathbf{y}_t), \quad (6)$$

where $f(\cdot)$ and $g(\cdot)$ are the paired visual encoder and text encoder of an align-based VLP model (*e.g.*, CLIP [40], ALBEF [29], Open-CLIP [11], and EVA-CLIP [19]), respectively.

When optimizing adversarial samples following Eqn. 5, this paper adopts PGD to update \mathbf{x}' with T iterations as below,

$$\mathbf{x}'_T = \mathcal{S}_\epsilon(\mathbf{x}'_{T-1} - \eta \cdot \text{sign}(\Delta_{\mathbf{x}'_{T-1}} \mathcal{L})), \quad \mathbf{x}'_0 = \mathbf{x}, \quad (7)$$

where η denotes step size, and \mathcal{S}_ϵ clips \mathbf{x}' into the ϵ -ball [35] of \mathbf{x} .

In Algorithm 1, we outline the whole pipeline of INSTRUCTTA. Initially, once decided an adversarial target text \mathbf{y}_t , we use the text-to-image model h_ξ and GPT-4 to “reverse” a target image \mathbf{x}_t and produce the reference instruction \mathbf{p}' , respectively. Furthermore, we augment the inferred instruction \mathbf{p}' with GPT-4 to form the instruction set Q . In each iteration, we randomly select instructions \mathbf{p}'_i and \mathbf{p}'_j from Q . Then, we update the adversarial example with PGD over Eqn. 5. Until the end of T step iterations, the final adversarial sample is obtained and used for attacking remote LVLMS.

4 Experiments

This section presents the experimental results of the proposed INSTRUCTTA on multiple victim LVLMs. We introduce the evaluation setup in § 4.1, and then present the results in § 4.2 followed by ablation study in § 4.3 and discussion in § 4.4.

4.1 Evaluation Setup

Datasets. The ImageNet-1K [15] comprises 3 subsets, including training, validation and test sets. We randomly select 1,000 images from the validation set to serve as the benign samples (\mathbf{x}) for the targeted attack. To establish the instruction-answer pairs as tested instructions and target texts, we adapt 11 instructions (see the supplementary material) from LLaVA-Instruct-150K [32] and employ GPT-4 to generate the corresponding answers. Specifically, we pick 1,000 images from the validation set of COCO [30], and for each image, we randomly select an instruction from these 11 instructions and utilize the GPT-4V [38] API to output the response. In addition, we use Stable Diffusion (h_ξ) to generate target images from the target texts, following [55].

Protocols. Following [55], we adopt CLIP-score (\uparrow) to evaluate the targeted attack performance, which calculates the semantic similarity between the generated response of victim LLM and the target text using CLIP text encoders. Additionally, we record the number of successful attacks (NoS) and attack success rate (ASR) by using GPT-4 to determine whether two texts have the same meaning. The prompt in this operation is as follows:

Attack success prompt
Determine whether these two texts describe the same objects or things, you only need to answer yes or no: <ol style="list-style-type: none"> 1. \mathbf{y}' 2. \mathbf{y}_t

where \mathbf{y}' denotes the output response of the adversarial example on the victim model, and \mathbf{y}_t is the target response.

Baselines. This paper provides evaluations on five victim LVLMs, including **BLIP-2** [28], **InstructBLIP** [14], **MiniGPT-4** [57], **LLaVA** [32], and **CogVLM** [46]. In detail, we select flan-t5-xxl², vicuna-7b-v1.1³, vicuna-v0-13b⁴, LLaMA-2-13B⁵ and vicuna-7b-v1.5⁶ as LLMs for BLIP-2, InstructBLIP, MiniGPT-4,

² <https://huggingface.co/google/flan-t5-xxl>

³ <https://huggingface.co/lmsys/vicuna-7b-v1.1>

⁴ <https://huggingface.co/Vision-CAIR/vicuna>

⁵ <https://huggingface.co/liuhaotian/llava-llama-2-13b-chat-lightning-preview>

⁶ <https://huggingface.co/lmsys/vicuna-7b-v1.5>

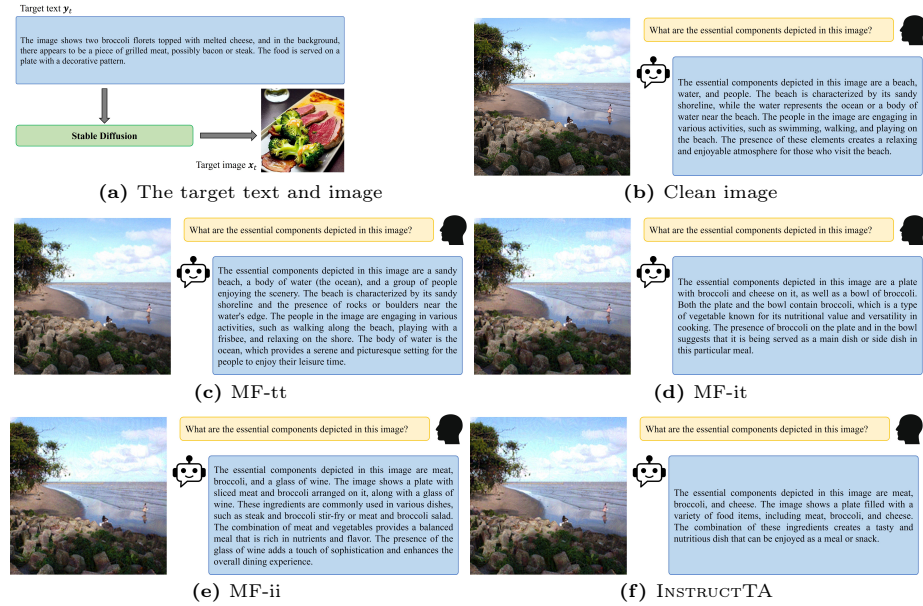


Fig. 4: Visualization examples of various targeted attack methods on InstructBLIP. "What are the essential components depicted in this image?" is a real instruction.

LLaVA and CogVLM⁷, respectively. For BLIP-2, InstructBLIP and MiniGPT-4, their visual encoders are all ViT-G/14 [51] borrowed from EVA-CLIP [19]. The vision encoders for LLaVA and CogVLM are built on ViT-L/14 [40] and EVA2-CLIP-E [43], respectively. To evaluate the targeted attack performance, INSTRUCTTA is compared with existing baselines, *i.e.*, **MF-tt**, **MF-it** and **MF-ii** [55]. MF-tt is a query-based black-box attack method that only accesses the input and output of the target model.

Implementation Details. All images are resized to 224×224 before feeding in substitute models and LVLMs. MF-it and MF-ii choose the same vision encoders as the victim LVLMs as surrogate models for targeted attacks. For INSTRUCTTA, we choose the vision encoder (ViT-G/14) and Q-Former from InstructBLIP as the surrogate model. In other words, ViT-G/14 and Q-Former are the visual encoder and projector in Fig. 1, respectively. For BLIP-2, InstructBLIP and MiniGPT-4, our surrogate models of INSTRUCTTA share the same vision encoders as the target models, regardless of the instruction-aware surrogate model or MF-it used in the dual targeted attack. For LLaVA and CogVLM, only MF-it in INSTRUCTTA (Eqn. 5) keeps the same vision encoder as the victim model. For PGD, η and T are set to 1 and 100, respectively. The maximum perturbation magnitude ϵ is set to 8. The settings of MF-tt, MF-it and MF-ii are all consistent with the original literature [55]. We implement all the evaluations using Pytorch 2.1.0 and run them on a single NVIDIA RTX A6000 GPU (48G).

⁷ <https://huggingface.co/THUDM/cogvlm-base-224-hf>

Table 1: Targeted attacks against victim LVLMs. A total of 1,000 clean images denoted as \mathbf{x} are sampled from the ImageNet-1K [15] validation set. For each of these benign images, a targeted text \mathbf{y}_t and a prompt \mathbf{p} are randomly assigned from our generated instruction-answer paired set (see § 4.1). Our analysis involves the computation of the CLIP-score (\uparrow) [40, 55] between the target texts and the generated responses of AEs on attacked LVLMs, which was performed using several CLIP text encoders and their ensemble. We also report the No. of successful attacks (NoS) within 1,000 adversarial samples, determined by GPT-4.

LVLm	Attack method	Text encoder (pretrained) for evaluation						NoS (\uparrow)
		RN50	RN101	ViT-B/16	ViT-B/32	ViT-L/14	Ensemble	
BLIP-2	Clean image	0.281	0.395	0.323	0.333	0.184	0.303	1
	MF-tt [55]	0.284	0.400	0.326	0.337	0.185	0.306	0
	MF-it [55]	0.533	0.634	0.575	0.581	0.469	0.559	401
	MF-ii [55]	0.536	0.634	0.575	0.583	0.471	0.560	414
	INSTRUCTTA	0.562	0.660	0.604	0.611	0.502	0.588	519
InstructBLIP	Clean image	0.329	0.450	0.358	0.361	0.246	0.349	1
	MF-tt [55]	0.332	0.452	0.361	0.363	0.249	0.351	1
	MF-it [55]	0.650	0.714	0.675	0.676	0.608	0.665	233
	MF-ii [55]	0.638	0.707	0.666	0.667	0.594	0.654	223
	INSTRUCTTA	0.683	0.740	0.709	0.708	0.645	0.697	300
MiniGPT-4	Clean image	0.324	0.448	0.348	0.351	0.244	0.343	2
	MF-tt [55]	0.332	0.455	0.353	0.356	0.243	0.348	0
	MF-it [55]	0.593	0.672	0.611	0.618	0.538	0.606	121
	MF-ii [55]	0.602	0.682	0.621	0.623	0.548	0.615	128
	INSTRUCTTA	0.633	0.701	0.650	0.654	0.578	0.643	164
LLaVA	Clean image	0.325	0.465	0.374	0.383	0.216	0.352	1
	MF-tt [55]	0.329	0.466	0.376	0.386	0.217	0.355	1
	MF-it [55]	0.368	0.502	0.418	0.424	0.268	0.396	32
	MF-ii [55]	0.360	0.496	0.407	0.415	0.256	0.387	30
	INSTRUCTTA	0.395	0.524	0.445	0.449	0.300	0.423	36
CogVLM	Clean image	0.301	0.425	0.319	0.334	0.208	0.318	4
	MF-tt [55]	0.307	0.432	0.327	0.342	0.212	0.324	8
	MF-it [55]	0.493	0.597	0.506	0.513	0.417	0.505	71
	MF-ii [55]	0.499	0.600	0.516	0.521	0.423	0.512	63
	INSTRUCTTA	0.528	0.624	0.539	0.545	0.452	0.537	103

4.2 Results

Targeted Attack Performance. As illustrated in Table 1, we transfer adversarial samples generated by different targeted attack methods to victim LVLMs and mislead them to produce target responses. For each adversarial example, when attacking an LVLm, the target text and the assigned instruction may be different from other adversarial examples, since we randomly selected 1000 pairs of target texts and instructions from our generated instruction-answer paired set (see § 4.1). Subsequently, we evaluate the similarity between the generated response \mathbf{y}' of the victim LVLm and the targeted text \mathbf{y}_t by utilizing diverse forms of CLIP text encoders, where $\mathbf{y}' = F(\mathbf{x}', \mathbf{p})$. In addition, we tabulate the count of successful targeted adversarial samples (NoS), as evaluated by GPT-4.

Table 1 reports the evaluation results of different targeted attack methods on BLIP-2, InstructBLIP and MiniGPT-4. We compare INSTRUCTTA with MF-tt, MF-it and MF-ii, which are the three recent attacks on LVLms. Overall, we

Table 2: Ablation study of the proposed method on BLIP-2. CLIP-score [55] is computed by ensemble CLIP text encoders. Attack success rate (ASR) is the ratio between the No. of attack successes and the total No. of samples.

Attack method	CLIP-score (\uparrow)	ASR (\uparrow)
INSTRUCTTA	0.588	0.519
INSTRUCTTA-woMF	0.574	0.472
INSTRUCTTA-woMFG	0.521	0.324

observe that INSTRUCTTA consistently outperforms MF-tt, MF-it and MF-ii in terms of CLIP score and NoS. In fact, it can be seen that MF-tt has almost the same results as the clean samples, indicating no promising targeted attack effect. In contrast, MF-it, MF-ii, and our method exhibit significant improvements over the clean samples on targeted attack results. This observation indicates the effectiveness of targeted attack methods against victim LVLMS.

Significantly, INSTRUCTTA surpasses MF-it and MF-ii in terms of CLIP-score and NoS, underscoring its superiority. These observations highlight the capacity of our method to enhance the transferability of targeted attacks on LVLMS. This is attributable to two factors. Firstly, we enhance the resilience of adversarial examples to diverse instructions, thereby bolstering their robustness. Secondly, our dual attack scheme extracts informative features that encompass both global and instruction-aware knowledge, thus facilitating precise targeted attacks.

Generalization of INSTRUCTTA. We argue that INSTRUCTTA exhibits a degree of generalization in attacking LVLMS, even when the vision encoder of the instruction-aware surrogate model differs from that of the target LVLMS. As evidenced in Table 1, the surrogate model employed is ViT-G/14 from EVA-CLIP [19], distinct from the ViT-G/14 and EVA02-bigE-14 utilized in LLaVA and CogVLM respectively. Despite this discrepancy, we observe that INSTRUCTTA outperforms previous methods in terms of targeted attack effectiveness. Hence, INSTRUCTTA can enhance its attack transferability beyond MF-it without necessitating the maintenance of an identical visual encoder to the victim LVLMS.

Visualization Examples. Fig. 3 has displayed a sample inferred instruction and its sibling instructions rephrased by GPT-4. It can be seen that the instruction inferred by GPT-4 is similar to the real instruction. The rephrased instructions are even more similar to the original sentence.

Moreover, we also provide some visual results of different attack methods on attacking InstructBLIP, as shown in Fig. 4. Overall, it can be observed that the generated response of our methods is closer to the target text.

4.3 Ablation Study

We also launched an ablation study to explore the contribution of major components in the proposed method. At this step, we conducted experiments on BLIP-2 with two key components ablated sequentially: 1) removing MF-it (denoted as

Table 3: Targeted attack performance for multiple perturbation budget ϵ .

Budget ϵ	Text encoder (pretrained) for evaluation						ASR (\uparrow)
	RN50	RN101	ViT-B/16	ViT-B/32	ViT-L/14	Ensemble	
2	0.406	0.516	0.451	0.458	0.326	0.431	0.127
4	0.510	0.613	0.552	0.558	0.445	0.535	0.349
8	0.562	0.660	0.604	0.611	0.502	0.588	0.519
16	0.570	0.669	0.610	0.617	0.509	0.595	0.605
64	0.575	0.673	0.616	0.623	0.516	0.600	0.604

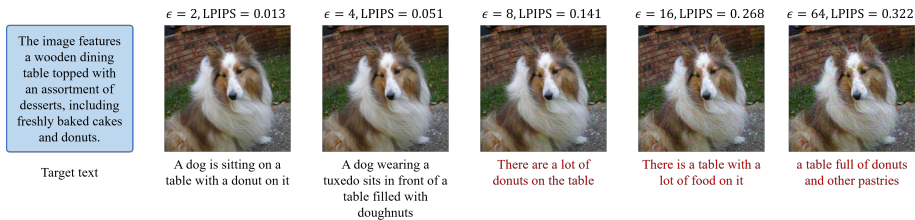


Fig. 5: To explore the impact of varying ϵ values within the INSTRUCTTA, we conducted experiments aiming to achieve different levels of perturbed images on BLIP-2, *i.e.*, referred to as the AE \mathbf{x}' . Our findings indicate a degradation in the visual quality of \mathbf{x}' , as quantified by the LPIPS [53] distance between the original image \mathbf{x} and the adversarial image \mathbf{x}' . Simultaneously, the effectiveness of targeted response generation reaches a saturation point. Consequently, it is crucial to establish an appropriate perturbation budget, such as $\epsilon = 8$, to effectively balance the image quality and the targeted attack performance.

INSTRUCTTA-woMF), and 2) launching optimization without MF-it nor GPT-4 for paraphrases (in accordance with Eqn. 3; denoted as INSTRUCTTA-woMFG).

The results are reported in Table 2. It is observed that the performances degrade when one or more parts are removed. In particular, the INSTRUCTTA-woMFG setting exhibits a success rate downgrading of over 19% in comparison to the complete INSTRUCTTA framework. Overall, we interpret the ablation study results as reasonable, illustrating that all the constituent components have been thoughtfully devised and exhibit congruity, culminating in an efficacious solution for the targeted attack.

4.4 Discussion

Effect of ϵ . To explore the effect of the perturbation magnitude ϵ on targeted attack performance, we study the attack results of INSTRUCTTA toward BLIP-2 under various ϵ . The results are reported in Table 3. It is evident that with ϵ increasing, both CLIP-scores and attack success rates rise, illustrating stronger attack performance. Nevertheless, it is seen that the attack performance becomes gradually saturated when ϵ is greater than 16. Moreover, as shown in Fig. 5, an overly large ϵ (*e.g.*, 16 and 64) has made the perturbation perceptible to naked eyes. Thus, we suggest to explore a proper ϵ for the targeted attack, *e.g.*,

Table 4: Targeted attack performance for different n .

Parameter n	Text encoder (pretrained) for evaluation						ASR (\uparrow)
	RN50	RN101	ViT-B/16	ViT-B/32	ViT-L/14	Ensemble	
1	0.560	0.658	0.600	0.606	0.498	0.584	0.504
5	0.560	0.657	0.600	0.606	0.498	0.584	0.504
10	0.562	0.660	0.604	0.611	0.502	0.588	0.519
50	0.562	0.659	0.601	0.607	0.499	0.586	0.529

Table 5: Average CLIP-score (\uparrow) between different versions of instructions. Each type of instruction has 1,000 samples.

Instruction	Rephrased instruction $\mathbf{p}'_{i/j}$	Real instruction \mathbf{p}
Inferred instruction \mathbf{p}'	0.943	0.829
Real instruction \mathbf{p}	0.828	1.000

$\epsilon = 8$, such that the attack performance can be effectively improved while the perturbation is imperceptible.

Effect of count n . In rephrasing prompt \mathbf{p}_r , we use $n - 1$ to control the number of instructions rephrased by GPT-4. With the original instruction, we totally collect n instructions to participate in the tuning for our targeted attack. To explore the effect of n on targeted attack performance, we perform INSTRUCTTA on BLIP-2 with varying n . The results are illustrated in Table 4. We can observe that CLIP scores are roughly the same for different n . It is worth noting that as n increases, the attack success rate (ASR) also increases. Therefore, increasing the number of paraphrased instructions can further improve ASR.

Assessment of Generated Instructions. To quantitatively evaluate the usability of the generated instructions, we collect a paraphrased instruction for each inferred instruction used in the main experiment and provide average CLIP-score values between them, as reported in Table 5. It is evident that there exists a high similarity score between the rephrased and the inferred instructions; moreover, the rephrased and the inferred instructions both show high similarity with the real instructions. We interpret the results as encouraging, demonstrating the high quality of employed instructions.

5 Conclusion, Ethics, and Mitigation

Our work highlights the vulnerability of LVLMs to adversarial attacks under a practical, gray-box scenario. INSTRUCTTA delivers targeted attacks on LVLMs with high transferability, demonstrating the importance of instruction-based techniques and the fusion of visual and language information in boosting adversarial attacks. The aim of our work is to enhance the resilience of LVLMs. Ethically, since we discovered adversarial examples, we minimized harm by (1) avoiding any damage to real users and (2) disclosing the detailed attacking process and methods used to find them in this paper. Overall, we believe that the

security of the LVLm ecosystem is best advanced by responsible researchers investigating these problems. Looking ahead, we envision the feasibility of launching various mitigation methods to improve the robustness of LVLms against adversarial attacks. For instance, we can leverage the adversarial training framework [35] to train LVLms with adversarial examples. We can also explore the possibility of incorporating adversarial training into the pre-training stage of LVLms or their vision encoders. Moreover, we can also explore detecting adversarial examples by leveraging the discrepancy between the instruction-aware features of the adversarial examples and the original images.

References

1. Akhtar, N., Mian, A.: Threat of adversarial attacks on deep learning in computer vision: A survey. *IEEE Access* **6**, 14410–14430 (2018)
2. Alayrac, J.B., Donahue, J., Luc, P., Miech, A., Barr, I., Hasson, Y., Lenc, K., Mensch, A., Millican, K., Reynolds, M., et al.: Flamingo: a visual language model for few-shot learning. *Advances in Neural Information Processing Systems* **35**, 23716–23736 (2022)
3. Awadalla, A., Gao, I., Gardner, J., Hessel, J., Hanafy, Y., Zhu, W., Marathe, K., Bitton, Y., Gadre, S., Sagawa, S., et al.: Openflamingo: An open-source framework for training large autoregressive vision-language models. *arXiv preprint arXiv:2308.01390* (2023)
4. Bai, J., Bai, S., Yang, S., Wang, S., Tan, S., Wang, P., Lin, J., Zhou, C., Zhou, J.: Qwen-vl: A versatile vision-language model for understanding, localization, text reading, and beyond. *arXiv preprint arXiv:2308.12966* (2023)
5. Bailey, L., Ong, E., Russell, S., Emmons, S.: Image hijacking: Adversarial images can control generative models at runtime. *arXiv preprint arXiv:2309.00236* (2023)
6. Biggio, B., Corona, I., Maiorca, D., Nelson, B., Šrndić, N., Laskov, P., Giacinto, G., Roli, F.: Evasion attacks against machine learning at test time. In: *Machine Learning and Knowledge Discovery in Databases*. pp. 387–402. Springer Berlin Heidelberg, Berlin, Heidelberg (2013)
7. Carlini, N., Wagner, D.: Towards evaluating the robustness of neural networks. In: *IEEE Symposium on Security and Privacy*. pp. 39–57. IEEE, San Jose, CA, USA (2017)
8. Chen, H., Zhang, H., Chen, P.Y., Yi, J., Hsieh, C.J.: Attacking visual language grounding with adversarial examples: A case study on neural image captioning. In: *ACL* (2018)
9. Chen, J., Guo, H., Yi, K., Li, B., Elhoseiny, M.: Visualgpt: Data-efficient adaptation of pretrained language models for image captioning. In: *CVPR*. pp. 18030–18040 (June 2022)
10. Chen, P.Y., Zhang, H., Sharma, Y., Yi, J., Hsieh, C.J.: Zoo: Zeroth order optimization based black-box attacks to deep neural networks without training substitute models. In: *ACM Workshop on Artificial Intelligence and Security*. pp. 15–26. Association for Computing Machinery, New York, NY, USA (2017)
11. Cherti, M., Beaumont, R., Wightman, R., Wortsman, M., Ilharco, G., Gordon, C., Schuhmann, C., Schmidt, L., Jitsev, J.: Reproducible scaling laws for contrastive language-image learning. In: *CVPR*. pp. 2818–2829 (2023)

12. Chiang, W.L., Li, Z., Lin, Z., Sheng, Y., Wu, Z., Zhang, H., Zheng, L., Zhuang, S., Zhuang, Y., Gonzalez, J.E., Stoica, I., Xing, E.P.: Vicuna: An open-source chatbot impressing gpt-4 with 90%* chatgpt quality (March 2023), <https://lmsys.org/blog/2023-03-30-vicuna/>
13. Chung, H.W., Hou, L., Longpre, S., Zoph, B., Tay, Y., Fedus, W., Li, Y., Wang, X., Dehghani, M., Brahma, S., et al.: Scaling instruction-finetuned language models. arXiv preprint arXiv:2210.11416 (2022)
14. Dai, W., Li, J., Li, D., Tiong, A.M.H., Zhao, J., Wang, W., Li, B., Fung, P., Hoi, S.: Instructblip: Towards general-purpose vision-language models with instruction tuning. arXiv preprint arXiv:2305.06500 (2023)
15. Deng, J., Dong, W., Socher, R., Li, L.J., Li, K., Fei-Fei, L.: Imagenet: A large-scale hierarchical image database. In: CVPR. pp. 248–255. IEEE (2009)
16. Dong, Y., Chen, H., Chen, J., Fang, Z., Yang, X., Zhang, Y., Tian, Y., Su, H., Zhu, J.: How robust is google’s bard to adversarial image attacks? arXiv preprint arXiv:2309.11751 (2023)
17. Dong, Y., Liao, F., Pang, T., Su, H., Zhu, J., Hu, X., Li, J.: Boosting adversarial attacks with momentum. In: CVPR. pp. 9185–9193. IEEE, Salt Lake City, UT, USA (2018)
18. Dosovitskiy, A., Beyer, L., Kolesnikov, A., Weissenborn, D., Zhai, X., Unterthiner, T., Dehghani, M., Minderer, M., Heigold, G., Gelly, S., et al.: An image is worth 16x16 words: Transformers for image recognition at scale. In: ICLR (2021)
19. Fang, Y., Wang, W., Xie, B., Sun, Q., Wu, L., Wang, X., Huang, T., Wang, X., Cao, Y.: Eva: Exploring the limits of masked visual representation learning at scale. In: CVPR. pp. 19358–19369 (2023)
20. Gao, L., Zhang, Q., Song, J., Liu, X., Shen, H.T.: Patch-wise attack for fooling deep neural network. In: ECCV. pp. 307–322. Springer (2020)
21. Gong, T., Lyu, C., Zhang, S., Wang, Y., Zheng, M., Zhao, Q., Liu, K., Zhang, W., Luo, P., Chen, K.: Multimodal-gpt: A vision and language model for dialogue with humans. arXiv preprint arXiv:2305.04790 (2023)
22. Goodfellow, I.J., Shlens, J., Szegedy, C.: Explaining and harnessing adversarial examples. In: ICLR. pp. 1–10. <http://OpenReview.net>, San Diego, CA, USA (2015)
23. Google: Google bard (2023), <https://bard.google.com/>
24. Gu, J., Jia, X., de Jorge, P., Yu, W., Liu, X., Ma, A., Xun, Y., Hu, A., Khakzar, A., Li, Z., et al.: A survey on transferability of adversarial examples across deep neural networks. arXiv preprint arXiv:2310.17626 (2023)
25. Ilyas, A., Engstrom, L., Athalye, A., Lin, J.: Black-box adversarial attacks with limited queries and information. In: ICML. pp. 2137–2146. PMLR, Stockholmmsäsan, Stockholm SWEDEN (2018)
26. Kurakin, A., Goodfellow, I., Bengio, S.: Adversarial machine learning at scale. In: ICLR. pp. 1–17. <http://OpenReview.net>, Toulon, France (2017)
27. Li, C., Gao, S., Deng, C., Xie, D., Liu, W.: Cross-modal learning with adversarial samples. In: NeurIPS (2019)
28. Li, J., Li, D., Savarese, S., Hoi, S.: Blip-2: Bootstrapping language-image pre-training with frozen image encoders and large language models. In: ICML (2023)
29. Li, J., Selvaraju, R., Gotmare, A., Joty, S., Xiong, C., Hoi, S.C.H.: Align before fuse: Vision and language representation learning with momentum distillation. In: NeurIPS. pp. 9694–9705 (2021)
30. Lin, T.Y., Maire, M., Belongie, S., Hays, J., Perona, P., Ramanan, D., Dollár, P., Zitnick, C.L.: Microsoft coco: Common objects in context. In: ECCV. pp. 740–755. Springer (2014)

31. Liu, A., Huang, T., Liu, X., Xu, Y., Ma, Y., Chen, X., Maybank, S.J., Tao, D.: Spatiotemporal attacks for embodied agents. In: ECCV. pp. 122–138. Springer (2020)
32. Liu, H., Li, C., Wu, Q., Lee, Y.J.: Visual instruction tuning. In: NeurIPS (2023)
33. Liu, Y., Chen, X., Liu, C., Song, D.: Delving into transferable adversarial examples and black-box attacks. In: ICLR (2017), <https://openreview.net/forum?id=Sys6GJqx1>
34. Lu, D., Wang, Z., Wang, T., Guan, W., Gao, H., Zheng, F.: Set-level guidance attack: Boosting adversarial transferability of vision-language pre-training models. In: ICCV. pp. 102–111 (2023)
35. Madry, A., Makelov, A., Schmidt, L., Tsipras, D., Vladu, A.: Towards deep learning models resistant to adversarial attacks. In: ICLR. pp. 1–28. <http://OpenReview.net>, Vancouver, BC, Canada (2017)
36. OpenAI: ChatGPT. <https://openai.com/blog/chatgpt> (2022)
37. OpenAI: Gpt-4 technical report. arXiv preprint arXiv:2303.08774 (2023)
38. OpenAI: Gpt-4v(ision) system card (2023), <https://openai.com/research/gpt-4v-system-card>
39. Papernot, N., McDaniel, P., Goodfellow, I., Jha, S., Celik, Z.B., Swami, A.: Practical black-box attacks against machine learning. In: ACM on Asia Conference on Computer and Communications Security. pp. 506–519. Association for Computing Machinery, New York, NY, USA (2017)
40. Radford, A., Kim, J.W., Hallacy, C., Ramesh, A., Goh, G., Agarwal, S., Sastry, G., Askell, A., Mishkin, P., Clark, J., et al.: Learning transferable visual models from natural language supervision. In: ICML. pp. 8748–8763. PMLR (2021)
41. Rombach, R., Blattmann, A., Lorenz, D., Esser, P., Ommer, B.: High-resolution image synthesis with latent diffusion models. In: CVPR. pp. 10684–10695 (2022)
42. Shayegani, E., Dong, Y.: Jailbreak in pieces: Compositional adversarial attacks on multi-modal language models. In: ICLR (2024)
43. Sun, Q., Fang, Y., Wu, L., Wang, X., Cao, Y.: Eva-clip: Improved training techniques for clip at scale. arXiv preprint arXiv:2303.15389 (2023)
44. Szegedy, C., Zaremba, W., Sutskever, I., Bruna, J., Erhan, D., Goodfellow, I., Fergus, R.: Intriguing properties of neural networks. In: ICLR. pp. 1–10. <http://OpenReview.net>, Banff, AB, Canada (2014)
45. Tang, R., Ma, C., Zhang, W.E., Wu, Q., Yang, X.: Semantic equivalent adversarial data augmentation for visual question answering. In: ECCV. pp. 437–453. Springer (2020)
46. Wang, W., Lv, Q., Yu, W., Hong, W., Qi, J., Wang, Y., Ji, J., Yang, Z., Zhao, L., Song, X., et al.: Cogvlm: Visual expert for pretrained language models. arXiv preprint arXiv:2311.03079 (2023)
47. Wang, Y., Hu, W., Dong, Y., Hong, R.: Exploring transferability of multimodal adversarial samples for vision-language pre-training models with contrastive learning. arXiv preprint arXiv:2308.12636 (2023)
48. Xu, X., Chen, X., Liu, C., Rohrbach, A., Darrell, T., Song, D.: Fooling vision and language models despite localization and attention mechanism. In: CVPR. pp. 4951–4961 (2018)
49. Yin, Z., Ye, M., Zhang, T., Du, T., Zhu, J., Liu, H., Chen, J., Wang, T., Ma, F.: Vlattack: Multimodal adversarial attacks on vision-language tasks via pre-trained models. In: NeurIPS (2023)
50. Yu, L., Rieser, V.: Adversarial textual robustness on visual dialog. In: ACL. pp. 3422–3438 (2023)

51. Zhai, X., Kolesnikov, A., Houlsby, N., Beyer, L.: Scaling vision transformers. In: CVPR. pp. 12104–12113 (2022)
52. Zhang, J., Yi, Q., Sang, J.: Towards adversarial attack on vision-language pre-training models. In: ACM MM. pp. 5005–5013 (2022)
53. Zhang, R., Isola, P., Efros, A.A., Shechtman, E., Wang, O.: The unreasonable effectiveness of deep features as a perceptual metric. In: CVPR (2018)
54. Zhang, S., Roller, S., Goyal, N., Artetxe, M., Chen, M., Chen, S., Dewan, C., Diab, M., Li, X., Lin, X.V., et al.: Opt: Open pre-trained transformer language models. arXiv preprint arXiv:2205.01068 (2022)
55. Zhao, Y., Pang, T., Du, C., Yang, X., Li, C., Cheung, N.M., Lin, M.: On evaluating adversarial robustness of large vision-language models. In: NeurIPS (2023)
56. Zhou, Z., Hu, S., Li, M., Zhang, H., Zhang, Y., Jin, H.: Advclip: Downstream-agnostic adversarial examples in multimodal contrastive learning. In: ACM MM. pp. 6311–6320 (2023)
57. Zhu, D., Chen, J., Shen, X., Li, X., Elhoseiny, M.: Minigt-4: Enhancing vision-language understanding with advanced large language models. arXiv preprint arXiv:2304.10592 (2023)

A Real Instructions

Here are the 11 real instructions adapted from LLaVA-Instruct-150K:

- What’s your interpretation of what’s happening in this picture?
- What is taking place in this scenario?
- Describe the image’s visual elements with extensive detail.
- Could you explain the key elements of this picture to me?
- What are the essential components depicted in this image?
- What does this picture represent?
- Could you provide more detail on the components of the image shown?
- Compose an elaborate depiction of the presented picture.
- Examine the picture thoroughly and with attention to detail.
- Provide a description of the image below.
- What can you observe occurring in this picture?

Table A6: Targeted attack performance with shuffled instructions.

LVLM	Attack method	Text encoder (pretrained) for evaluation						NoS (↑)
		RN50	RN101	ViT-B/16	ViT-B/32	ViT-L/14	Ensemble	
BLIP-2	Clean image	0.275	0.397	0.319	0.328	0.177	0.299	2
	MF-tt	0.277	0.400	0.320	0.331	0.177	0.301	3
	MF-it	0.529	0.634	0.574	0.578	0.465	0.556	419
	MF-ii	0.529	0.634	0.570	0.578	0.463	0.555	419
	INSTRUCTTA	0.556	0.658	0.597	0.604	0.493	0.582	561

B Cross-Instruction Transferability

To explore the cross-instruction transferability of targeted attacks, we shuffle the instruction-answer paired set given certain semantic similarities between the 11 instructions. The results on BLIP-2 are reported in Table A6. We can see that our INSTRUCTTA shows the best targeted attack performances in terms of CLIP-score and NoS. Hence, the adversarial examples generated by our method have superior cross-instruction transferability.

C Source Code

The source code is available at <https://github.com/xunguangwang/InstructTA>.